marine ecology

| RESEARCH ARTICLE OPEN ACCESS

Seasonal Changes of Size Spectra of the Benguela Offshore Mesopelagic Ecosystem Compartment in Relation to Primary Production

Heino O. Fock[1] | Henrike Andresen[1] | Javier Díaz Pérez[2] | Tim Dudeck[3] | Gabriela Figueiredo[4] | Thierry Frédou[5] | Dawit Y. Ghebrehiwet[6] | Cristina González-García[7] | José M. Landeira[2] | Simone Lira[4] | Emilio Marañón[8] | Leandro Nole Eduardo[9] | Ralf Schwamborn[4]

[1]Thünen, Inst. Of Sea Fisheries, Bremerhaven, Germany | [2]Universidad de las Palmas de Gran Canaria, Instituto de Oceanografía y Cambio Global, Las Palmas, Spain | [3]Leibniz Centre for Tropical Marine Research (ZMT), Bremen, Germany | [4]Department of Oceanography, Federal University of Pernambuco (UFPE), Recife, Brazil | [5]Department of Fisheries and Aquaculture, Universidade Federal Rural de Pernambuco (UFRPE), Recife, Brazil | [6]Department of Forestry, Fisheries & the Environment, Fisheries Branch, Cape Town, South Africa | [7]Instituto Español de Oceanografía, IEO-CSIC, Centro Oceanográfico de Vigo, Vigo, Spain | [8]Departamento de Ecología y Biología Animal, Universidade de Vigo, Vigo, Spain | [9]Institut de Recherche Pour le Développement (IRD), Sète, France

Correspondence: Heino O. Fock (heino.fock@thuenen.de)

ABSTRACT

Seasonal differences in marine size spectra of micronekton at the shelf-ocean interface of the northern (NBUS) and southern Benguela upwelling system (SBUS) in Feb–Mar 2019 and Sep–Oct 2021 were analysed for mesopelagic fishes and total micronekton, the latter also including invertebrates. A resource dependent population model based on the metabolic theory of ecology (MTE) containing resource and temperature terms and a term representing a transfer function was applied to test three different types of size spectra slope estimates. The model fitted best with linear slopes calculated of log-binned averaged community biomass (LBNbiom method), while maximum likelihood and quantile regression estimates proved less effective. The best model for total micronekton contained significant effects both for resource term and transfer function, but not for temperature, and was 3.6 times more effective explaining the data than a non-MTE model. Normalized biomass size spectra (NBSS) slopes of the total micronekton were in the theoretical range between -0.80 and -1.37, where the near-equilibrium slope of -0.80 was obtained for the SBUS under oligotrophic conditions in 2021. Seasonally, NBSS slopes were steeper in the NBUS than in the SBUS. The slopes for the fishes' subcomponents ranged from -0.23 to -0.92, where values > -0.75 fall outside the theoretical range, suggesting that selecting taxonomic subsets for size spectrum analysis is problematic. The importance of the productivity regime shaping the biomass spectrum directly through the resource level and indirectly through the transfer function is highlighted. For mesopelagic fishes, generation time and fecundity are applied to explain slopes > -0.75.

1 | Introduction

Abundance-biomass allometry relationships viz. size spectra are among the most widely used macro-ecological patterns to describe changes in the functioning of ecological communities (Gaston and Blackburn 2000; Kerr and Dickie 2001; Cohen et al. 2003), rooted in the observations that "roughly equal concentrations of material occur at all particle sizes … from bacteria to whales" in the ocean (Sheldon and Parsons 1967; Sheldon et al. 1972). The background for these models lies in the scaling of metabolism in relation to body size. The energy equivalence relationship (Allen et al. 2002) states that when all species within a certain trophic level (TL) share a common resource and have the same metabolic requirements, energy allocation should be the same across the body mass range considered, that is, independent of body mass M. Hence, in accordance to the metabolic theory of ecology (MTE), basic metabolic rate scales as $M^{0.75}$ and abundance as $M^{-0.75}$ (Brown and Gillooly 2003; Brown et al. 2004; Arim et al. 2011), so that within a trophic level energy use is scaled as $M^{0.75} \cdot M^{-0.75} = M^0$ (energy equivalence rule) and subsequently the biomass spectrum $B(M)$ as $M^{0.25}$, that is, the product of average body mass M times abundance (Jennings and Mackinson 2003). A common resource means all zooplankton feed on the same contingent of phytoplankton, all planktivorous fishes feed on the same pool of zooplankton etc. MTE does not consider the scaling of energy use to be temperature dependent. Across trophic levels, energy is lost according to trophic transfer efficiency (TTE) between predator and prey trophic levels separated by the predator–prey-mass-ratio (PPMR) leading to an additional correction of $M^{-0.25}$, with TTE equal to 0.1 and PPMR equal to 10,000. Hence, in accordance to Sheldon's observation the community biomass spectrum $B(M)$ is scaled as M^0 and community abundance spectrum $N(M)$ as M^{-1} (Equation 1, see Fock and Czudaj 2019), and $B(M)$ denotes the spectral density of B in size class M:

$$B(M) \propto aM^{\frac{\log 10(\text{TTE})}{\log 10(\text{PPMR})} + 0.25} \qquad (1)$$

Further dividing by M leads to normalized spectra, where the normalized biomass spectrum $B_{\text{norm}}(M)$ scales as M^{-1} (normalized biomass size spectra, NBSS) and the normalized abundance spectrum $N_{\text{norm}}(M)$ as M^{-2} with a as normalization constant (equation 13 in Brown et al. 2004).

Implicit to this model is that size is the only determinant of function and that energy is transferred at the same transfer efficiency and the same size relationship between predator and prey (PPMR) for all trophic levels (TL) so that on a log–log scale, the abundance-body mass relationship in Equation (1) is linear. However, functional traits as specific adaptations may override size as the only determinant. The $M \sim$ TL relationship may be reversed in that in the marine realm large filter-feeding microphages (tunicates) or planktivorous organisms (baleen whales, whale sharks) exist, so that the increase in TL is not necessarily correlated with body mass M. Omnivory may further weaken strong $M \sim$ TL and PPMR relationships, considering the prevalence of omnivory in marine pelagic ecosystems (Thompson et al. 2007). Hence, the size dependence is a simplification (Rossberg 2012). In turn, Cohen et al. (2003) showed that including food web properties in size-dependent modeling, that is, the body mass rank of a species which helps to model its trophic vulnerability, allows linking all trophic variables to body size and abundance.

The slope of the size spectrum changes with resource levels (Rodriguez and Mullin 1986; Gaedke 1992; González-García et al. 2023), mass-dependent changes, and reversion in PPMR (Trebilco et al. 2016; Tsai et al. 2016), and changes in metabolic rates due to life history or ontogenetic stages (Rossberg 2012). Thus, different scaling regimes with different slopes may appear in different size range domains (Arim et al. 2011), so that extrapolations from the linear log–log plot might not be justified. Further differences may appear due to taxonomic selection since many meta-ecological studies are based on taxonomic subsets only (Gaston and Blackburn 2000). With regard to the provision of ecosystem resources, ecosystem type may play a role in that in marine systems complex hydrography can lead to mixing of water masses of different productivities and thus resource levels (e.g., frontal systems, transport through eddies, water mass filaments in upwelling regions).

We apply size spectrum analysis in the context of MTE to analyze seasonal differences in size spectra for the taxonomic subset of mesopelagic fishes and the entire community of micronekton in the offshore Benguela upwelling system (BUS) (water depth > 500 m) and investigate the effects of changes in temperature and resource supply. Within a population, equilibrium abundance at the level of carrying capacity scales as $M^{-0.75}$ (Brown et al. 2004). Brown et al. (2004) and Savage et al. (2004) used this approach to describe the effects of temperature T and resource availability R on equilibrium abundance N:

$$N(M) \propto f(R) \, M^{-0.75} \, e^{\frac{E}{kT}} \qquad (2)$$

where k is the Boltzmann constant and E is the activation energy. MTE suggests that NBSS are continuous and linear (Brown et al. 2004). In contrast, with variability in resource availability, abundance-body mass relationships may become dome shaped (Arim et al. 2011) with consecutive peaks indicative of feeding interactions between prey abundant in a certain size class and its predators (Thiebaux and Dickie 1992, 1993; Kerr and Dickie 2001), also described as cascading effects (Rossberg et al. 2019).

2 | Material and Methods

2.1 | Study Area

The BUS along the west coast of South Africa, Namibia, and Angola is one of the world's four productive eastern boundary upwelling systems. The BUS is separated into a northern (NBUS) and southern part (SBUS) by the Lüderitz permanent upwelling cell at 26° S. The northern limit is defined by the Angola-Benguela front at 19° S, and the southern limit at 34° S. The BUS current system is composed of wind-driven northerly surface currents and poleward undercurrents, where NBUS and SBUS each maintain separate undercurrent cells (Duncombe Rae 2005). They are influenced by two different source water masses, namely the high-salinity,

oxygen-poor, and nutrient-rich South Atlantic Central Water (SACW) in the north and the low-salinity, oxygen-rich, and nutrient-poor Eastern South Atlantic Central Water (ESACW) in the south (Hutchings et al. 2009; Jarre et al. 2015), with subsequent differences in primary production in the offshore environment (Table 1). Depending on productivity, turbidity was much higher in the NBUS; subsequently, the amplitude of daily vertical migration of the acoustic backscattering layer 2019 was from the surface to ca 400 m in the NBUS and from the surface to ca 500 m in the SBUS (no data 2021), with a less dense deep scattering layer remaining at depth during the night. Additional leakage from the Agulhas current leads to entrainment of Indian Ocean water, especially into the SBUS, while tropical water penetrates through the Angola-Benguela front into the NBUS. At the shelf-ocean interface, the oceanic mesopelagic community mixes with shelf components, while some mesopelagic species, that is, the pseudoceanic species, have adopted a specific life history to build up significant shelf populations as well (*Lampanyctodes hectoris*, *Maurolicus walvisensis*). A detailed study of the Benguela mesopelagic off-shore ecosystem component (Duncan et al. 2022) reveals two main assemblages with typical myctophid species *Diaphus hudsoni*, *Lampanyctus australis*, and *Diaphus dumerilii* in the NBUS, and *Diaphus meadi* in the SBUS. Important mesopelagic predators are stomiids *Chauliodus sloani* in the SBUS and *Stomias boa* in the NBUS. In 2019, the austral summer was sampled, while in 2021, the austral spring was sampled, the latter coinciding with a strong so-called Benguela Niño, where +1°C SST anomalies were observed in the region from July to October 2021 (Illig and Bachèlery 2023). On the shelf (water depth < 500 m), the pelagic ecosystem is characterized by a "wasp-waist" community, dominated by a few species of "small pelagics" (sardines, anchovies, round herring) that control both the lower trophic levels (zooplankton) and the higher trophic levels, such as birds, predatory fish, and marine mammals (Cury et al. 2000).

2.2 | Sampling and Sample Collection Strategy

Samples were collected during two seasons, austral summer during the R/V Meteor cruise 153 from 19 February to 12 March 2019 (M153, Ekau 2019), and austral spring during the R/V Sonne cruise 285 from 13 September to 9 October 2021 (SO285, Rixen et al. 2021). A rectangular midwater trawl (RMT) 8 m²-net was deployed (Baker et al. 1973) with a non-grading mesh size of 4.5 mm, and a net bucket cod-end with a mesh size of 1.0 mm. The effective tow duration of each haul was about 30 min with a ship speed of 2.5–3.0 knots. The RMT was deployed to a sampling depth of ca 500 m as a double oblique tow covering both the migrating as well as non-migrating parts of the deep scattering layer (Duncan et al. 2022). Only stations with more than 500 m bottom depth were considered in this analysis (= offshore habitat). The micronekton was split into two broader categories, that is, mesopelagic fish including larvae and invertebrate micronekton, the latter also including macrozooplankton and jellyfishes. Size spectra were calculated both for the mesopelagic fish and for the total of mesopelagic fish and invertebrate micronekton and zooplankton (= total micronekton). Taxonomic analysis for fishes and processing was followed by earlier established protocols (Fock and Czudaj 2019; Duncan et al. 2022). Individual

TABLE 1 | Availability of samples from the northern and southern Benguela upwelling system for size spectrum analysis and environmental characteristics. NPP is the average of the first sampling month and the two preceding months.

Region and season	Number of invertebrate stations (i.e., samples)	Total number of invertebrate micronekton specimens	Total number of fish larvae	Number of stations (i.e., samples) of mesopelagic fishes	Total number of mesopelagic fishes (adult)	Invertebrate biomass (g m⁻³)	Fish biomass (larvae and adult, g m⁻³)	Net primary production (NPP, mg C m⁻² day⁻¹).	In situ temperature at 10 m depth (T10, °C)
NBUS 2019	5	64,930	0	9	920	0.023	0.0051	1450	20.16
SBUS 2019	5	32,688	3691	6	248	0.004	0.0016	1100	20.3
NBUS 2021	5	18,302	158	7	513	0.008	0.0052	1690	16.46
SBUS 2021	5	8047	115	5	545	0.002	0.0027	622	15.53

weights were obtained as wet weights, either measured directly or calculated from specific length-weight relationships (see Czudaj et al. 2022). Invertebrate micronekton wet weight was weighed directly. For gelatinous macro- and megazooplankton (Scyphomedusae, Hydromedusae, Siphonophora, Salpidae, Tunicata, Chaetognatha), a weight conversion factor from Palomares and Pauly (2009) was applied to account for the higher water content of gelatinous tissues as compared to fish and crustacean tissues.

Sea surface temperature was derived from in situ measurements (CTD-casts) at 10 m depth (T10) and below, because satellite-derived data were not capturing the seasonal gradient properly. Primary production data were averaged over the first sampling month plus the preceding 2 months in accordance with water residence times of ca 100 days (Liu et al. 2019). Production data were acquired from the chlorophyll-based Vertically Generalized Production Model (VGPM) (Behrenfeld and Falkowski 1997) from http://www.science.oregonstate.edu/ocean.productivity.

2.3 | Size Spectrum Analysis

Edwards et al. (2017) identified five different methods to analyze size spectra that were fairly accurate; these can be assigned to two model classes, that is, linear models based on log-binning with normalization using biomass and the analysis of power law models with maximum likelihood parameter estimation. Model outputs from both model classes are applied to investigate the MTE population dynamic model (Equation 2).

2.3.1 | Linear Regression on a Log–Log Scale

Log–log models were about the first applications to visualize size dependencies of ecological communities (Platt and Denman 1977). Data were binned at octave scale, where body mass M doubles between subsequent size classes. As NBSS represent a class of models of type Y/X versus X, spurious correlations must be tested for (Blanco et al. 1994; Brett 2004; Williams et al. 2022). A randomization test was applied with $n = 999$. A correction for the intercept, as suggested by Blanco et al. (1994) was not applied, since the focus was on the analysis of slopes.

Two specifications were applied. Firstly, log-binning with normalization using biomass is applied to samples pooled per region and season with linear averaging per size class and functional subset (fishes, invertebrate micronekton), analogous to the LBNbiom method (Edwards et al. 2017) already applied to mesopelagic fishes (Fock and Czudaj 2019). Binning is carried out in $\log_2$-bins, that is, octave scale (Platt and Denman 1977) with bin midpoints 0.5, 1, 2, 4 g etc.

Pooling samples and averaging allows including station spectra that contain size bins with zero biomass, so that minimum abundance values smaller than the lower detection range may be encountered. Pooling samples over an annual cycle, over a specific range of the water column or spatially is common practice (Sheldon et al. 1972; Rossberg 2012; Fock and Czudaj 2019). LBNbiom was calculated from the maximum value of the spectrum to the last consecutive non-zero value in the data ensemble,

so that zero size classes are not treated as missing values. For the slopes of the subset of mesopelagic fishes, in addition to the rule of the maximum value, a lower limit size class of 1 g was applied.

The second specification was a quantile regression on an ensemble of individual station data, that is, without pooling samples, on the reasoning that the upper limit of the station-wise data distribution may represent a stronger predictive relationship than the mean (Cade and Noon 2008). The upper body mass limit was set to 64 g for this regression to avoid zero values.

For pelagic gear, the lower limiting detection range of abundance of specimens is 10^{-6} to 10^{-7} ppm (Witek and Krajewska-Soltys 1989). Thus, a 1 g specimen ($\approx 1\,\text{cm}^3$) should be present at least 1 time in $10^7\ \text{m}^3$ of volume. As sampling volumes for a single sample ranged between 40,000 and 80,000 m^3, that is two orders of magnitude smaller, the limiting density for 1 g specimens therefore is about $10^{-5}\,\text{m}^{-3}$. This is included as a reference line to indicate how the size spectra performed at low densities, and the respective limit for 10 g specimens would be 10^{-4} specimens m^{-3}. This limit consideration is important since LBNbiom estimates become biased toward lower density values if relatively too large (= rare) specimens are included, whereas this method performs well in an optimal body mass size range (Edwards et al. 2017).

2.3.2 | Power Law Distributions and Pareto Distributions

With dome-shaped patterns in the spectrum as pointed out above, binning into size classes may under- or overweigh certain body mass ranges. The second model class, power law distributions rooted in Pareto distribution models (Vidondo et al. 1997; Newman 2005; Edwards 2008; White et al. 2008; Arim et al. 2011) may overcome this shortcoming. They basically describe an abundance spectrum $N(m)$ for which the density function in relation to individual body mass m is (note: not size class M):

$$N(m) \propto Cm^{-\mu} \tag{3}$$

For each chosen minimum limit $m_{\min}$ for all specimens i with $m_i > m_{\min}$ in an assemblage, the Maximum Likelihood Estimate of power μ is (Edwards et al. 2007; Arim et al. 2011)

$$\hat{\mu} = 1 + n \left[\sum_{n=1\ to\ i} \log\left(\frac{m_i}{m_{\min}} \right) \right]^{-1} \tag{4}$$

which can be resolved to

$$\hat{\mu} = 1 - \frac{1}{\log\left(m_{\min}\right) - \frac{\sum_n \log(m_i)}{n}} \tag{5}$$

Plotting of estimates μ as a function of $m_{\min}$ and the cumulative density function of $m \geq m_{\min}$ (CDF) allows to break up the entire scaling pattern into scaling regions, indicative of regime shifts between size classes (Arim et al. 2011). The MLE slopes in Table 2 were rescaled as $\mu = \mu_{\text{MLE}} + 1$ (Luiz and Edwards 2011)

TABLE 2 | Normalized biomass size spectrum slopes of the different models and data subsets. Fish—mesopelagic fishes.

Data compartment	Region and season	LBNbiom μ	Quant reg 95% μ 0.25 g threshold	MLE $\mu_{MLE}+1$, 0.25 g threshold
Total micronekton	NBUS_2019	−1.37	−1.79	−0.8
Total micronekton	SBUS_2019	−1.04	−1.10	−0.84
Total micronekton	NBUS_2021	−1.07	−1.42	−0.9
Total micronekton	SBUS_2021	−0.80	−0.99	−1.12
Fishes	NBUS_2019	−0.92		
Fishes	SBUS_2019	−0.79		
Fishes	NBUS_2021	−0.23		
Fishes	SBUS_2021	−0.57		
Fishes	NBUS_2019 – 1 g lower limit	−0.99		
Fishes	SBUS_2019 – 1 g lower limit	−0.77		
Fishes	NBUS_2021 – 1 g lower limit	−0.96		
Fishes	SBUS_2021 – 1 g lower limit	−0.91		

to make them comparable to LBNbiom and quantile regression slopes.

2.4 | The Population Density Model

We tested for seasonally resolved slopes from the three specifications of slope modeling in combination with seasonally resolved primary production and temperature data. We applied the MTE equation for equilibrium population density under the assumption (Equation 2) that if all populations were in equilibrium, the slopes should scale as −0.75 for populations without predation or where predation is independent of body size (see Arim et al. 2011). Extending with $M^{0.75}$ removes the equilibrium scaling from the right-side terms in Equation (2) so that a transfer function (transfer through predation and losses due to other interactions) with exponent $\Delta\mu = \mu + 0.75$ is retained. Here, μ is the observed slope of the NBSS considering the formal equivalence of abundance spectrum slope and NBSS slope. The model function is obtained after taking natural logs, with l being the respective size class and k the community (season by region):

$$0.75\ln\left(M_{l,k}\right) + \ln N_{l,k} = \ln\left(f\left(R_k\right)\right) + E\frac{1}{kT_k} + \ln M_{l,k}^{\Delta\mu_k} + \text{factor (Region)}$$

(6)

In MTE, the transfer function $\Delta\mu$ is equivalent to the term $\frac{\log \text{TTE}}{\log(\text{PPMR})}$. Additionally, a region effect is included as factor (NBUS or SBUS). The left-side term of Equation (6) can be interpreted as equilibrium weighted abundance. We apply three different formulations for the resource level $f(R)$, which is supposed to be a linear term (Brown et al. 2004; Savage et al. 2004). Firstly, an intercept and an exponent in the log-model are included equivalent to a power function $f(R) = aR^b$, secondly without an intercept in the log-model equivalent to a power term $f(R) = R^b$, and finally, treating it as linear term $f(R) = aR$ with exponent 1, that is, division by R and retaining

an intercept in the log-model. Models are selected upon the Akaike information criterion (AIC), where lower values indicate a better model. Burnham et al. (2011) pointed out, that not only the best model should be considered but that models with minor AIC differences can be likewise plausible and thus should be evaluated by means of their evidence ratio V of Akaike weights w(AIC), that is, $V = w_1(\text{AIC}) / w_2(\text{AIC})$ exemplified for two models 1 and 2 (Al Halwachi et al. 2004). The differences in slopes for the selected models were tested according to Paternoster et al. (1998).

3 | Results

3.1 | Data

Sea surface temperatures in March 2019 were considerably higher than in September 2021, but did not differ much between NBUS and SBUS. In 2019, NBUS and SBUS SST were 20.16°C and 20.3°C, as compared to 16.49°C and 15.79°C in 2021, respectively. Offshore primary production was always higher in the NBUS as compared to the SBUS (Table 1).

Less samples were analyzed for the invertebrate component than for mesopelagic fishes (Table 1), and only those samples with both invertebrate micronekton and mesopelagic fishes had been analyzed for the quantile regression and power law distribution approach. In 2021, average abundance per sample of micronekton/zooplankton was considerably lower than in 2019 (Table 1).

3.2 | Normalized Biomass Size Spectra

LBNbiom size spectra showed strong differences between seasons, region, and micronekton components considered. Although fishes mainly shape the spectrum above a body mass of 1 g (vertical line in Figure 1 panels), below 1 g body
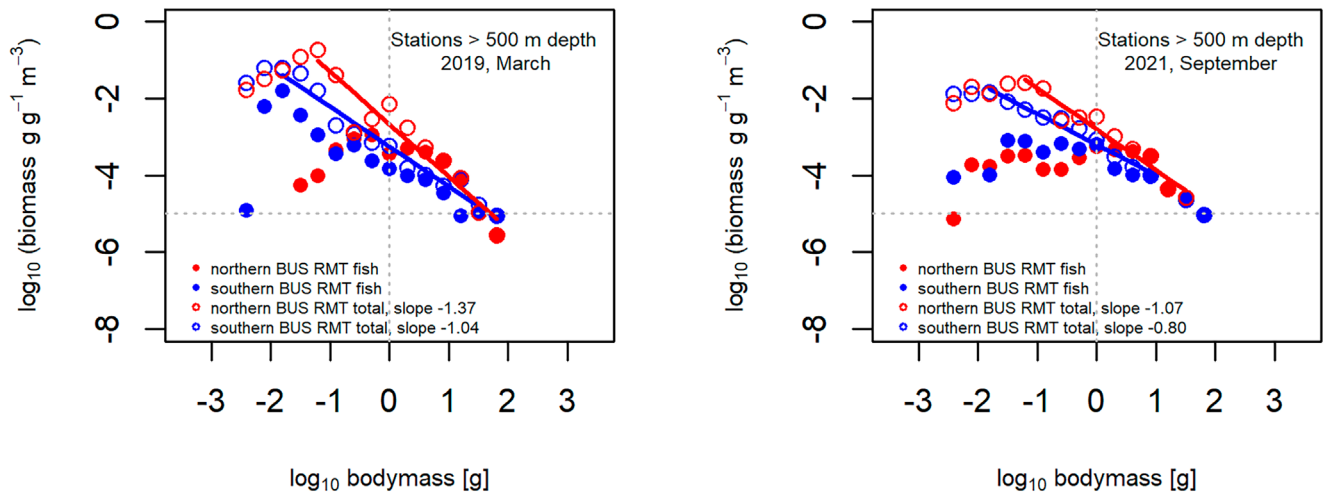
FIGURE 1 | NBSS for total micronekton community and mesopelagic fishes separately, slopes refer to total micronekton assemblage. LBNbiom method applied. Hatched horizontal line represents the 10^{-7} ppm detection threshold.

mass invertebrates dominate by several orders of magnitude of normalized biomass. Only in 2019 in the SBUS, relatively high normalized biomass of fish larvae <1 g was found, mainly due to high abundances of especially anchovy larvae (*Engraulis encrasicolus*); however, still one order of magnitude lower than the invertebrate normalized biomass. Normalized biomass was always higher in the NBUS as compared to the SBUS. It is evident that the LBNbiom slope of the total micronekton community only approximates the variability of the normalized biomass of the different size classes. In 2019, high values were found in the NBUS at size classes of 1 and 0.03125 g, the former generated by Decapoda (amongst others *Gennadas* spp., Sergestidae, Syllaspidae) and the latter by Euphausiacea, amongst others *Euphausia hanseni*. For mesopelagic fish and fish larvae on their own, only the size spectrum of SBUS 2019 appears to resemble a linear pattern, whereas the fish size spectra of NBUS 2019 and of both regions in 2021 appear like truncated cones, composed of a flat top of inner section and steeper flanks. The vertebrate size classes not well represented in the flat top in turn are filled in by respective invertebrate size classes, resulting in overall fairly linear models.

After inspecting Figure 1, the LBNbiom slopes appear nevertheless as a reasonable proxy for the differences in total micronekton size spectra (Table 2). All slopes were significantly different from random so that there is no Y/X versus X confounding problem (Figure S2). The slopes are steeper in the NBUS than in the SBUS in both seasons, and for both subsystems, steeper in 2019 than in 2021. The same applies to the slopes obtained from quantile regression; however, the slopes are steeper than LBNbiom slopes (Figure 2, Table 2). The sample size for MLE estimation of slopes is presented in Table 1. The evolution of μ_{MLE} while changing the minimum size over which the sample is aggregated (x_{min} in Figure 3, also Figures S3–S5) shows that slopes, except for the SBUS 2021 (Figure S5) do not stabilize around a $\log_{10}$ body mass of 0. In particular, the numerical increase in mostly invertebrate abundance below 0.25 g body mass is associated with a steepening of slopes (Figure 3). To account for this instability, a cut-off value for x_{min} of 0.25 g was chosen.
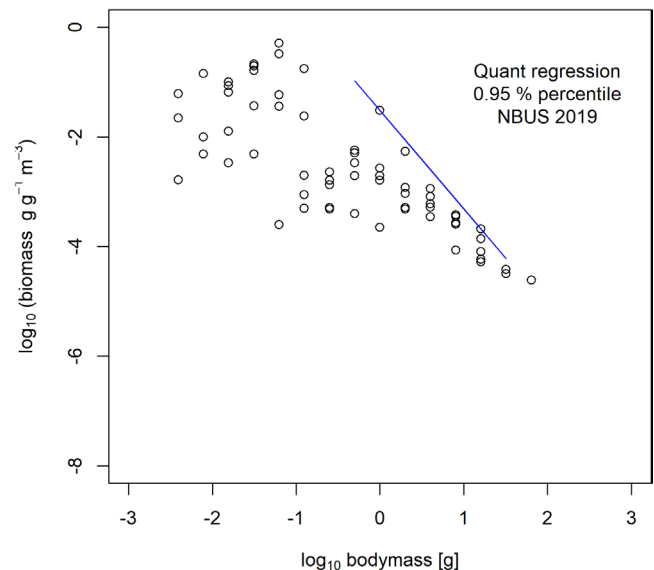

FIGURE 2 | The quantile regression interpretation of normalized biomass size spectrum slope of unpooled data for 5 stations, northern Benguela upwelling system offshore component, 2019.

The order of MLE slopes was opposite to the order of both slopes of LBNbiom and quantile regression, that is, the highest value for μ_{MLE} corresponded to the lowest LBNbiom and quantile regression slopes, and vice versa. However, the MLE plots reflected the variability shown in the LBNbiom plots by means of multiple scaling regions in the CDF plots.

The slopes for the fishes' subcomponents were less steep, ranging from −0.23 to −0.92 (Table 2), where values >−0.75 fall outside the theoretical range. The relationship to biomass is equivocal for total micronekton and mesopelagic fishes. Although total micronekton biomass was negatively related to LBNbiom slopes, this did not apply to mesopelagic fishes and fish larvae (Figure 4). However, the *p*-values suggest that the relationship for mesopelagic fishes and fish larvae was not significant.
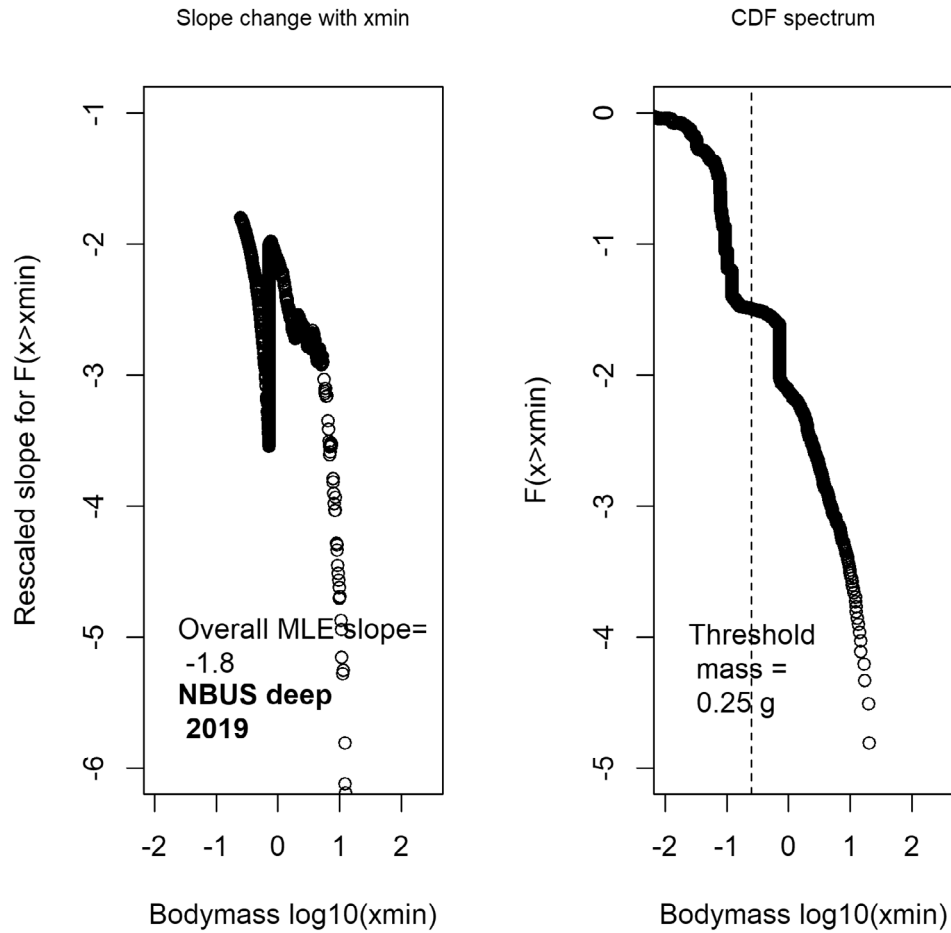
FIGURE 3 | Evolution of μ_{MLE} and corresponding cumulative density distribution in relation to minimum size $x_{\min}$ of total micronekton for NBUS 2019.
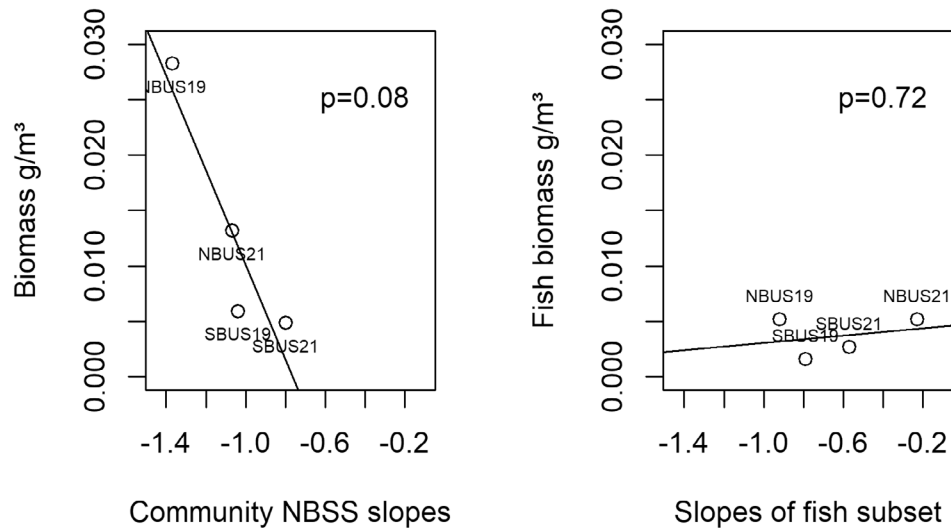

FIGURE 4 | LBNbiom slopes and biomass relationships for total micronekton community and mesopelagic fishes separately. Biomass calculated as sum of wet weight from size classes 0.0156–128 g for respective ecosystem components (see Table 1).

3.3 | Resource and Temperature Dependence of Size Spectra Slopes

The differently calculated slopes are evaluated in terms of their performance in the population density model. For total micronekton, LBNbiom slope estimates performed best (Table 3, models 3, 5, and 6) as compared to models 7–18 (for full suite of models see Figure S1). LBNbiom slopes for NBUS and SBUS were significantly different in 2019 ($p = 0.028$) and 2021 ($p = 0.016$, Table 2). The lowest AIC of 149.7 was indicated

TABLE 3 | Parameter estimates and model diagnostics of selected best NBSS models calculated. Best performing models were calculated with the LBNbiom method. For full suite of models see Table S1. Fish – mesopelagic fishes.

| | | | | | | Parameter estimates | | | | |
Model type	Slopes' model	AIC	w(AIC)	Model p	r²	a	ln(NPP)	1/kT	ln (M$^{\Delta b}$)	Region
Model 3— aR^b + transfer function—Region	LBNbiom	151.7	0.190	0.002	0.22	−37.8	+0.98*	+0.60	+0.09*	
Model 5— R^b + transfer function—Region	LBNbiom	152.2	0.142	< 0.001	0.98		+0.68●	- 0.30***	+0.08*	
Model 6— aR + transfer function—Region	LBNbiom	149.7	0.515	0.014	0.13	−38.4●		+0.60	+0.09*	
Fish Model 20— aR^b—transfer function + Region	LBNbiom	83.4	0.287	0.05	0.15	−2.25	−1.06	+0.06		−1.28*
Fish Model 24— aR + transfer function—Region	LBNbiom	82.9	0.365	0.01	0.20	−70.3**		+1.37**	+0.53*	

Note: Significance levels: $p < 0.1$ (●), $p < 0.05$ (*), $p < 0.01$(**) and $p < 0.001$ (***).

for model 6, which is the representation of Equation (2) with a resource term of $f(R) = aR$. The effect of factor *Region* (NBUS or SBUS) was not contained in model 6. The Akaike weights indicate that this model was $0.515/0.190 = 2.7$ times better than model 3 and 3.6 times better than model 5. In model 5, the formulation of the resource term appears unreasonable, despite high values for r^2 and significance level. Models 3 and 6 are similar, in that firstly the exponent for the resource component in model 3 was close to 1 (0.92), and secondly the parameter estimates for temperature were very similar (rounded 0.60 in both cases) although this term was not significant. Model 3 had a significant parameter estimate for b for $f(R) = aR^b$, whereas model 6 had a marginally significant parameter for a for $f(R) = aR$. That indicates that the resource function in both models has a significant impact, together with the remaining scaling $\Delta\mu$, while temperature is not significant. Nevertheless., the suggested temperature scaling of 0.60 in models 3 and 6 lied in the range of reported values of 0.43 (fishes) to 0.83 (invertebrates) (Brown et al. 2004). This positive relationship also appeared in bivariate plots for the fishes' subcomponent, but not for the total micronekton where it was negative (see Figures S6 and S7). This negative relationship also appeared in model 5, but the direction of the effect was not as expected, since MTE predicts that the carrying capacity should decline with increasing T meaning a positive slope for 1/kT. In models 3, 5 and 6 for the total micronekton assemblage, the transfer function was significant, indicating that the term $\hat{M}\frac{\log TTE}{\log(PPMR)}$ was important to understand changes in NBSS slopes.

Only LBNbiom models were analyzed for mesopelagic fishes and larvae given the results for total micronekton. For models 19–24, the maximum to last consecutive non-zero value selection was applied, representing the bulk of fish abundance across the truncated flat sections, while for models 25–30, the cut-off was set to 1 g to analyze whether the steeper flanks corresponded better to the population density model. The former models fitted better to the population density model; and again, model 24, representing Equation (2), is performing 1.3 times better than the next best model 20. The interesting difference between models 20 and 24 is that model 20 had almost no temperature scaling (parameter estimate = 0.06), a significant region term but no remaining scaling. This is similar to the community analysis of Duncan et al. (2022) identifying water mass properties and thus regions NBUS/SBUS as a significant term to distinguish communities in the BUS. In turn, model 24 had significant terms for temperature scaling, for a of $f(R) = aR$, as well as for remaining scaling. The parameter estimate for temperature scaling was relatively high (1.37) and had a strong positive effect also in bivariate analysis, which also applied to primary production (Figure S7).

4 | Discussion

Samples were taken from two seasons in two different years in the BUS, representative of the pelagic assemblages at the interface between shelf and open ocean. As such, they contain a mixture of genuine shelf components (e.g., krill) and—except for pseudoceanic species—genuine open ocean components (e.g., mesopelagic fishes). The shelf-ocean interface is an important spawning and nursery habitat, with small-scale frontal systems providing retention cells or good feeding conditions for fish larvae (Tiedemann et al. 2017). Eventually, the SBUS assemblage in 2019 was numerically dominated by anchovy larvae. These larvae are transported to their SBUS nursery grounds from their spawning grounds off the southern tip of South Africa (Ragoasha et al. 2019). The Benguela jet current along the shelf

edge in SBUS carries them some 400 km in a northerly direction. Spawning takes place from October to March, with peak spawning in December (Mullon et al. 2003). This makes the SBUS distinctive from its northern Benguela counterpart and the other major eastern boundary upwelling systems for which spawning and nursery grounds of small pelagics overlap.

Several methods have been proposed to analyze biomass size spectra, amongst others Reduced-Maximum-Axis techniques (Griffiths 1999) and other ways to bin data and conduct regressions (Edwards et al. 2017). Based on ecological reasoning, we chose three methods, that is, two regression techniques either looking at pooled samples representative of the mean state or at maximum values indicated by quantile regression. The MLE method was applied to overcome caveats suggested for binning methods (Edwards 2008; Edwards et al. 2020). The number of individuals, especially for the vertebrate component, was not very high (10^2–10^3 per region and season, Table 1). Fock and Czudaj (2019) worked with samples obtained with larger nets and analyzed more than 20,000 fishes for mesopelagic size spectra. Size range selected and sample size, however, influence the performance of NBSS methods. Blanco et al. (1994) showed that LBNbiom slopes become flat when calculated from too small sample sizes, and Edwards et al. (2017) indicated that with the inclusion of numerically overrepresented larger specimens, slopes also become more flat. To overcome the latter, we considered the detection limit of 10^{-6} to 10^{-7} ppm suggested by Witek and Krajewska-Soltys (1989) to evaluate the NBSS plots, while the problem of small sample sizes for vertebrates, to some degree, was solved by pooling samples. But even with the total assemblage considered, the MLE slope plots did not perform well. Hence, with larger sample sizes, MLE slope estimates would have probably been improved.

The slopes derived from different size spectra methods were applied to run the population density model outlined by Savage et al. (2004) to test temperature and resource availability effects. Different resource functions were tested, and the best performing models in terms of AIC both for total micronekton and separately for mesopelagic fishes and fish larvae were in accordance with the population density model (Brown et al. 2004; Savage et al. 2004) with a resource term $f(R) = aR$ and a positive effect for $1/kT$ (Table 3, models 6 and 24, full suite of models in Table S1). Looking at NBSS shapes and the relationship to biomass, LBNbiom estimates performed better than quantile regression and MLE estimates, and secondly, total micronekton performed better than the models for the subset of mesopelagic fishes and fish larvae. With regard to biomass, there was a fairly strong relationship between LBNbiom slopes observed for the entire community and biomass (Figure 4), while no relationship appeared for the fishes' subset. The parameter estimates for the resource function for the entire community were fairly significant in all cases, and the positive relationship also appeared in the bivariate plots. Although scaled in the appropriate range of magnitude, that is, +0.60, the activation energy E of the temperature effect was not significant. The temperature effect E is considered to lie between +0.43 and +0.83 and to be positive (Brown et al. 2004; Savage et al. 2004), that is, with increasing temperature due to increased metabolic stress the carrying capacity will decline. The energy effect for the mesopelagic fishes and fish larvae subcomponent was higher, that is, +1.37, which

was probably not calculated correctly due to sample size constraints. Of course, for animals that for some degree undertake daily vertical migrations, SST might also not be the right temperature proxy. Recalculating model 6 with the average temperature from surface to 100 m depth instead of SST resulted in a slightly inferior model, that is, model p-value was 0.015 as compared to 0.014, and the AIC weight decreased to 0.471 as compared to formerly 0.515 while model r^2 was the same, so settings in favor of SST were retained. The importance of temperature to govern mesopelagic assemblage structure regionally is probably not high, given that—also depth stratified—temperature was not significant both for the Benguela and the Mauritanian upwelling system to explain this (Duncan et al. 2022, 2024).

The LBNbiom slopes of the total micronekton agree with the energy equivalence rule of the MTE ranging from −0.80 to −1.37. The value of −0.75 is considered the limit when predation is size independent (Arim et al. 2011) and populations are at equilibrium (Brown et al. 2004; Savage et al. 2004). The value of −0.80 coincided in the SBUS in 2021 with very low rates of primary production averaged over a 3-month period. With increasing primary production rates, the slopes steepened. This steepening of slopes with suggested increased productivity was also shown for mesopelagic fishes in the eastern tropical Atlantic (Fock and Czudaj 2019). This is opposite to marine plankton, where for Atlantic phytoplankton a steepening has been observed with decreasing trophic status (González-García et al. 2023). For zooplankton, NBSS slopes in the late winter bloom of the Canary Current offshore system were less steep than for the less productive stratified season (Couret et al. 2023). This could indicate that ecosystem components each have a specific reaction pattern.

The LBNbiom models did not perfectly fit the NBSS, and the MLE plots indicated multiple scaling regimes for each of the assemblages. The CDF plots showed steeper increases of F(x) for $x_{min} < 0.25$ g except for SBUS 2021. Only in the latter case, the MLE slope reached a fairly stable value. Figure 4 indicates that the invertebrate and the fish assemblages responded differently to the different productivity regimes, and that the invertebrate faction may respond more rapidly to changes in nutrient supply, that is, the spectra indicated relatively more biomass in smaller size classes in NBUS 2019 and 2021 and SBUS 2019, but not in SBUS 2021. As compared to fishes, this invertebrate response, for example, for euphausiids (Werner et al. 2015), depends on shorter generations times t_B, which according to MTE are scaled to M as $t_B \sim M^{0.25}$ (Brown et al. 2004). Considering that in the analysis of size spectra time scales of biomass change relevant to the observation (seasonal, annual) interfere with time scales relevant for growth, the latter ranging from days to 10s of days for zooplankton (Zhou 2006), allows to reconcile our observations with the equilibrium model. In this context, the term $\frac{\log TTE}{\log(PPMR)}$ on the one side quantifies the transfer function $\Delta\mu$, on the other side it is indicative of the system departure from equilibrium. With a trophic transfer efficiency (TTE) of 0.1 and PPMR at 10,000, this term becomes −0.25 yielding a predicted NBSS slope of −1. With more efficient energy transfer and no change in PPMR, slopes should become larger than −1. In turn, with reduced TTE, slopes should become steeper, that is, with a TTE of 0.05 and a PPMR of 1000 NBSS slope μ should be at—1.20. For the SBUS 2021 assemblage, the slope was larger than −1 indicating

increased efficiency near equilibrium (LBNbiom slope = −0.8), the CDF plot did not show excess invertebrate biomass below a body mass limit of $x_{min} < 0.25\,g$ (Figure S5), associated with lowest primary production and lowest invertebrate biomass of all 4 cases measured (Table 1). On the other side, for NBUS 2019 the slope was smallest indicating reduced efficiency (LBNbiom slope = −1.37), the CDF plot showed a steep increase of biomass at $x_{min} < 0.25\,g$ (Figure 3), and invertebrate biomass was highest in the range selected (Table 1). Fish biomass in both systems was seasonally associated with larger community slopes, and was higher in the NBUS as compared to the SBUS (Figure 4). Thus, reconciling model and observations into a dynamic interpretation of size spectra changes, the increase in lower trophic level biomass (shorter generation times) could be explained by a fast initial response to seasonally increased nutrients (Figure 5.1). Starting from a near-equilibrium state with a stage 1 NBSS representative of SBUS 2021 with a flat CDF plot (Figure 5.1), a nutrient pulse would trigger the increase of abundance of smaller species, and the corresponding LBNbiom figure would indicate two domes at positions A1 and B1 in Figure 5.1 with an intermittent NBSS with steeper slope, where position A1 indicates the biomass increase and B1 is a regression artifact because the increase of fish biomass would not happen simultaneously. This could explain the structure observed in the LBNbiom figures with biomass peaks around 0.05, 1 and 10 g in the NBUS and less pronounced, for the SBUS (Figure 1). At continuous supply level, increased invertebrate biomass propagated through the food web would lead to higher biomass for higher trophic levels, and with a stable increased nutrient level, a potential stage 2 equilibrium would be reached (Figure 5.2). However, due to both seasonal variability and dynamic mixing processes at the Benguela shelf-ocean interface with residence times of coastal waters < 100 days (Liu et al. 2019), a stable stage 2 NBSS is unlikely in particular for ecosystem components with a generation time $t_B > 100$ days. The extent of the seasonal effect is reflected in the differences in community biomasses 2019 to 2021 (Figure 4), which is large for the NBUS but small for the oligotrophic offshore SBUS. The transfer to higher trophic levels is reflected in the average fish biomass, where generally higher fish biomass occurred in the NBUS as compared to the SBUS (Figure 4). Within-system comparisons reveal, that the increase in fish biomass is delayed relative to the increase of invertebrate biomass, since in both systems higher fish biomass was associated with lower invertebrate biomass indicating that generation time t_B to build up abundance is a critical factor (Figure 4). Thus, considering a single nutrient pulse means that after the end of the pulse the invertebrate abundance would return to previous levels A2 while abundance of organisms with higher t_B would bump up to a value B3 with a new intermittent NBSS slope (Figure 5.3). As mesopelagic fishes are an unfished resource offshore, there is no further extraction except natural mortality. This could explain the observed slopes for the fishes' subcomponents in the range > −0.75 that would fall outside the theoretical range predicted by MTE. Therefore, selecting taxonomic subsets for size spectrum analysis is problematic. In order to evaluate step 5.3, further NBSS data of mesopelagic fishes from Fock and Czudaj (2019) are plotted together with the BUS data (Figure 6). Slope values > −0.75 for the subset of mesopelagic fishes are no artifact, since in both data sets, slope values > −0.75 appeared at the low NPP range investigated, and for BUS only, also at high NPP, indicative of the bump-up pattern at B3. Fock and Czudaj (2019)
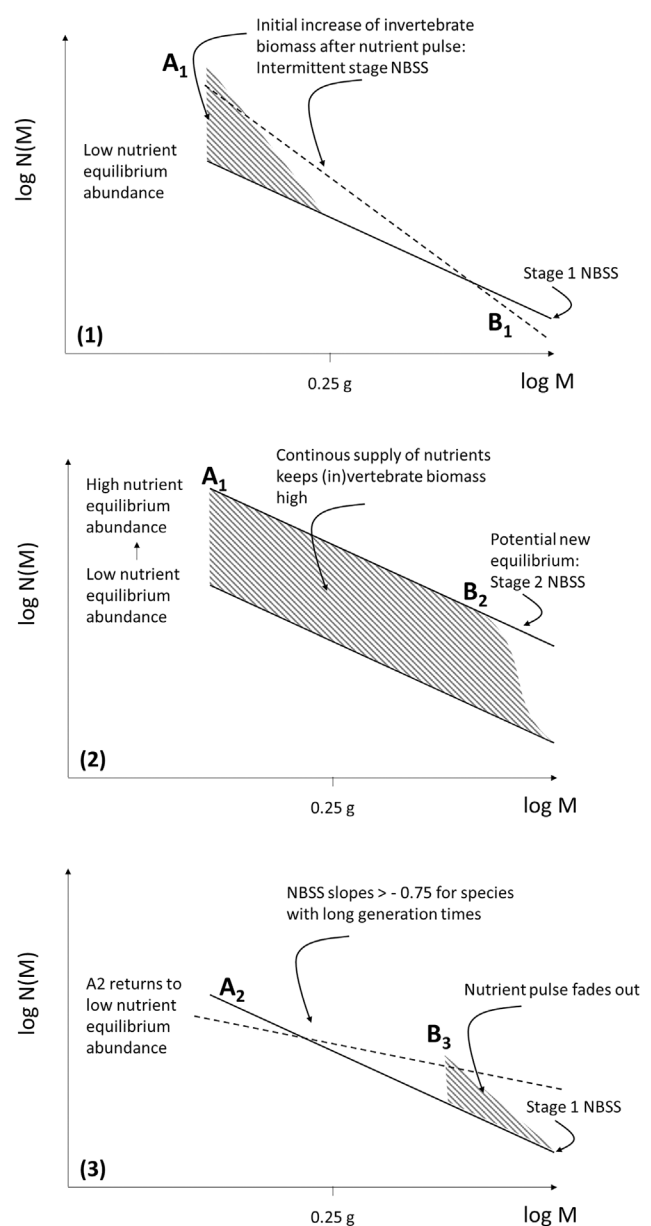

FIGURE 5 | Schematic diagram of changes of NBSS structure after nutrient pulses for different ecosystem components depending on generation time, (1) Initial increase after nutrient pulse of invertebrates with short generation time, (2) approaching a potential new equilibrium with continuously high nutrient input, and (3) progression of the initial increase of invertebrate biomass to organisms with higher body mass and longer generation times, after the nutrient pulse has ceased. Intermittent NBSS hatched, equilibrium NBSS with solid lines.

attributed slope differences to productivity changes in general, but did not provide an explicit explanation for values > −0.75. The B3 bump-up further indicates, that the mesopelagic fishes do not produce a sufficient number of offspring under oligo- and eutrophic conditions. The only case where fish larvae fit fairly into the size spectrum was the SBUS 2019, however, these were from small pelagics, that is, anchovy, and not from mesopelagic species. In fact, mesopelagic fish typically possess low fecundity and spawn in batches (Knorrn et al. 2023; Andresen et al. 2024), and therefore are less capable of reacting timely to short term pulses of food supply.
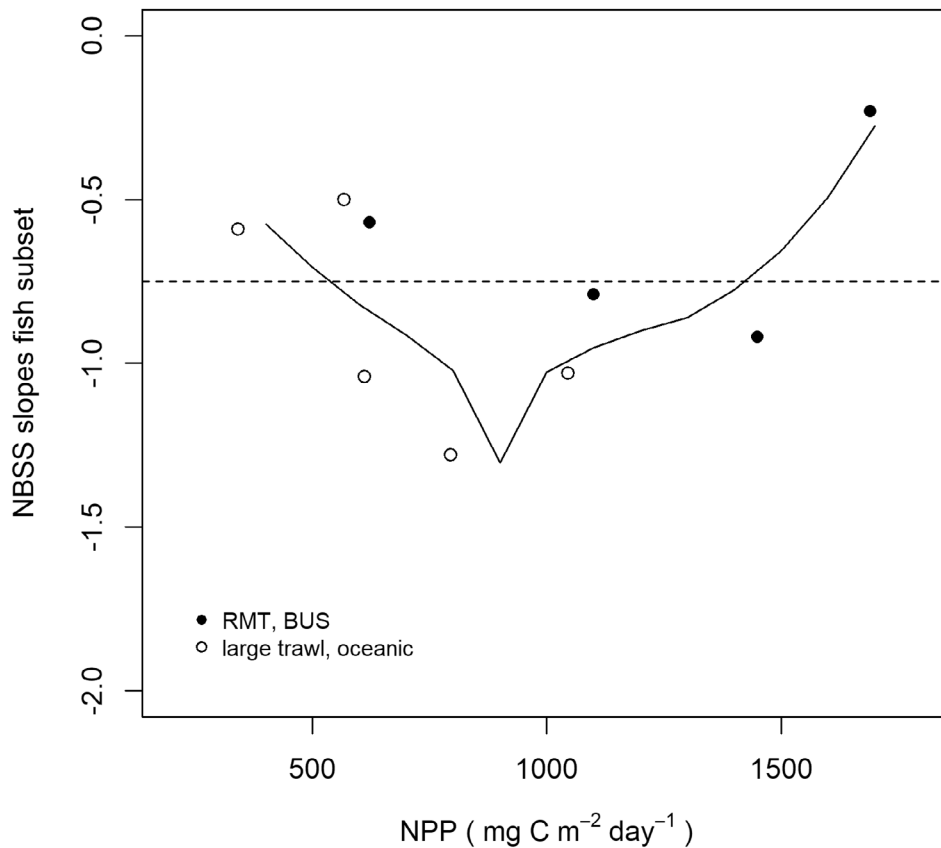
FIGURE 6 | Relationship between NBSS slopes and net primary production for the subset of mesopelagic fishes and fish larvae for the Benguela upwelling system (BUS) sampled with an RMT net and for published data of the historical tropical, subtropical and temperate, as well as tropical and subtropical North Atlantic from 2015 (Fock and Czudaj 2019). Seasonal NPP calculated for oceanic stations in the same way as described in the text. For the historical assemblages, NPP from 2006 were retrieved to account for changes in recent decades. Fitted line is a loess smoother. The horizontal hatched line indicates the equilibrium slope value of −0.75.

The interpretation of the transfer function in terms of transfer efficiency depends both on trophic transfer efficiency (TTE) and predator–prey-mass-ratio (PPMR). PPMR is a statistical concept, pointing at the average ratio of predator to prey mass (Brown et al. 2004). In upwelling areas, it can be expected that TTE is low due to significant sedimentation of organic material out of the pelagic system. This is evidenced by means of very high levels of sedimentary organic carbon in the NBUS (e.g., Emeis et al. 2018). Thus, the parameter estimate of the transfer function $\Delta\mu$ can be interpreted as a reduction in transfer rate of biomass differing from steady state by size of $M^{\Delta\mu*\text{parameter estimate}}$ to yield the abundance measured. Compared to $M^{-0.25}$ and a fish body mass of $M = 10\,\text{g}$ as baseline, the SBUS 2021 is +45.8% more efficient as compared to a reduced efficiency of—58.6% in the NBUS 2019. This could also be understood as a change in recycling efficiency or recycling loops of organic matter within a community. As such, Zhou (2006) showed that the number of recycling loops n in a community is related to NBSS slope μ as $n = \frac{1+\eta}{\eta*\mu}$, where η is assimilation efficiency of ingested food which varies from 0.6 (Andersen and Beyer 2015) to 0.8–0.85 (Kerr and Dickie 2001) for fishes. The number of recycling loops can be further understood as an increase in food chain length and in marine zooplankton is associated with oligotrophic ecosystem conditions (Armengol et al. 2019), which defines a link between surface trophic state and NBSS equilibrium conditions. The importance of surface production for diversity of deep-sea

fishes was shown (Fock 2009), indicating that surface production is propagated vertically throughout the water column.

The parameter estimates for $\Delta\mu$ ranged between 0.08 and 0.09 and thus did not account for the full value of $\Delta\mu$. Alternatively, this could indicate a temperature effect on the mass-dependent scaling of energy use. Lindmark et al. (2019) showed how a temperature-dependent component can be added to the scaling μ of metabolism, that is, $\mu_0 + c(T - T_0)$. Based on the energy equivalence rule with energy use scaled as M^0, abundance must scale accordingly as $-(\mu_0 + c(T - T_0))$ (Savage et al. 2004). Thus, a positive c (the parameter estimate for $\Delta\mu$ was positive and <1 in models 3, 5, 6 and also 24) would indicate that metabolism demands increase faster with temperature for large relative to small specimens, with an opposite effect on abundance. This alternative interpretation, however, could only explain the increase in biomass for small M seen in NBUS 2019 and 2021 and SBUS 2019 by a reduced predation effect by larger micronekton, meaning that in 2019, with increased temperatures and relatively lower biomasses of mesopelagic fishes, predation pressure was reduced in both subsystems, leading to higher invertebrate abundance. This would imply a negative parameter estimate for 1/kT, that is, equilibrium weighted abundance in particular for lower M would increase with temperature, a case that was shown for model 5. However, the non-MTE model 5 was 3.6 times less effective in explaining the data than model 6.

The low SBUS primary production rate in 2021 followed the seasonal cycle, but was also influenced by the 2021 Benguela Nino (Illig and Bachèlery 2023) which in the SBUS led to a decline in productivity opposite to the NBUS, with an increase of upwelling activity (Rouault and Tomety 2022). In the NBUS, increased inflow from the Angola basin must also be considered (Rouault et al. 2007), probably adding allochthonous assemblage components to the NBUS assemblage. This is often observed in terms of tropical species occurring in the subtropical NBUS (Duncan et al. 2022, own observations for 2021).

Whereas the transfer function for the total micronekton was always negative, that is, the LBNbiom slope was smaller than -0.75, for the subset of the mesopelagic fish this term was positive for the 2021 assemblages in models 19–24 where no lower size limit was applied. Opposite to the bump-up hypothesis, in terms of $\frac{\log TTE}{\log(PPMR)}$ positive values only are possible if PPMR becomes smaller than 1. This unlikely case (possible exceptions for instance like Chiasmodontidae (Herring 2002) were not present in our samples) indicates that the transfer function in models 19–24 has little ecological meaning. Interestingly, the second-best model 20 was without transfer function. The only significant term in this model was a region effect, in line with the observation by Duncan et al. (2022), that water mass affiliation was a significant factor in structuring NBUS and SBUS mesopelagic assemblages.

MTE as a theory has been challenged with the argument that its allometric scaling represents empirical relationships rather than universal laws (del Rio 2008; Price et al. 2012). Thus, MTE may be tested in several ways, amongst which are to evaluate its simplifications or to test its predictions (Price et al. 2012). In fact, when confronting the data with different models for the resource function, model specifications in line with the MTE proved to perform better than alternative models. Our results highlight the importance of the productivity regime in shaping the biomass spectrum through the resource function and by affecting the transfer function of the mass-dependent scaling. Near-equilibrium conditions of the MTE population model were found in the 2021 season of the SBUS under oligotrophic conditions. The MLE and the corresponding CDF plots allowed us to understand departures from near-equilibrium as a response to nutrient pulses in terms of relatively faster population growth of species with shorter generation times (Figure 5). Simplifications of the MTE, as pointed out for the deviations from the $M \sim TL$ relationship, likely do not confound the present analysis, given the similarities in assemblage structure between NBUS and SBUS in the two periods considered.

Author Contributions

H.O.F.: conceptualization (lead); field survey and sample analysis (equal), writing – original draft (lead); formal analysis (lead). J.D.P.: sample analysis (equal) writing – original draft (equal). H.A., T.D., G.F., T.F., D.Y.G., C.G.G., J.M.L., S.L., E.M., L.N.-E., R.S.: conceptualization (equal), writing – original draft (equal).

Acknowledgements

Disclosure

Scientific significance statement: The transition from open ocean to shelf ecosystems has not been investigated yet in terms of micronekton size spectra, especially not for productive upwelling systems. Likewise, the MTE has rarely been applied to build models to test the effects of resource availability, trophic transfer, and temperature on abundance spectra. Data from the northern and southern BUS are used to investigate these effects and furthermore, investigate alternative formulations of the resource function in line with and different from MTE. Our results highlight the importance of the productivity regime in shaping the biomass spectrum. Model specifications in line with the MTE proved to perform better than their competitors.

Conflicts of Interest

The authors declare no conflicts of interest.

Data Availability Statement

Composition data available at PANGAEA (Fock and Duncan 2024) and NBSS data available at ZENODO (Fock et al. 2024). Hydroacoustic data have been published by Dudeck and Ekau (2022).

References

Al Halwachi, H. K., D. S. Yakovlev, and E. S. Boek. 2004. "AIC Model Selection Using Akaike Weights." *Psychonomic Bulletin & Review* 11: 192–196.

Allen, A. P., J. H. Brown, and J. F. Gillooly. 2002. "Global Diversity, Biochemical Kinetics, and the Energetic-Equivalence Rule." *Science (New York, N.Y.)* 297: 1545–1548.

Andersen, K. H., and J. E. Beyer. 2015. "Size Structure, Not Metabolic Scaling Rules, Determines Fisheries Reference Points." *Fish and Fisheries* 16: 1–22. https://doi.org/10.1111/faf.12042.

Andresen, H., L. N. Eduardo, M. P. Olivar, et al. 2024. "Mesopelagic Fish Traits: Functions and Trade-Offs." *Fish and Fisheries* 26: 83–103. https://doi.org/10.1111/faf.12867.

Arim, M., M. Berazategui, J. M. Barrenche, L. Ziegler, M. Zarucki, and S. R. Abades. 2011. "Determinants of Density-Body Size Scaling Within Food Webs and Tools for Their Detection." *Advances in Ecological Research* 45: 1–39. https://doi.org/10.1016/B978-0-12-386475-8.00001-0.

Armengol, L., A. Calbet, G. Franchy, A. Rodríguez-Santos, and S. Hernández-León. 2019. "Planktonic Food Web Structure and Trophic Transfer Efficiency Along a Productivity Gradient in the Tropical and Subtropical Atlantic Ocean." *Scientific Reports* 9: 1–19. https://doi.org/10.1038/s41598-019-38507-9.

Baker, A. d. C., M. R. Clarke, and M. J. Harris. 1973. "The N.I.O Combination Net (RMT 1+8) and Further Developments of Rectangular Midwatertrawls." *Journal of the Marine Biological Association of the United Kingdom* 53: 167–184.

Behrenfeld, M. J., and P. G. Falkowski. 1997. "Photosynthetic Rates Derived From Satellite-Based Chlorophyll Concentration." *Limnology and Oceanography* 42: 1–20.

Blanco, J. M., F. Echevarría, and C. M. García. 1994. "Dealing With Size-Spectra: Some Conceptual and Mathematical Problems." *Scientia Marina* 58: 17–29.

Brett, M. T. 2004. "When Is a Correlation Between Non-Independent v Ariables 'Spurious'?" *Oikos* 105: 647–656. https://doi.org/10.1111/j.0030-1299.2004.12777.x.

Brown, J. H., and J. F. Gillooly. 2003. "Ecological Food Webs: High-Quality Data Facilitate Theoretical Unification." *Proceedings of the National Academy of Sciences of the United States of America* 100: 1467–1468. https://doi.org/10.1073/pnas.0630310100.

Brown, J. H., J. F. Gillooly, A. P. Allen, V. M. Savage, and G. B. West. 2004. "Toward a Metabolic Theory of Ecology." *Ecology* 85: 1771–1789. https://doi.org/10.1890/03-9000.

Burnham, K. P., D. R. Anderson, and K. P. Huyvaert. 2011. "AIC Model Selection and Multimodel Inference in Behavioral Ecology: Some Background, Observations, and Comparisons." *Behavioral Ecology and Sociobiology* 65: 23–35. https://doi.org/10.1007/s00265-010-1029-6.

Cade, B. S., and B. R. Noon. 2008. "A Gentle Introduction to Quantile Regression." *Frontiers in Ecology and the Environment* 1: 412–420.

Cohen, J. E., T. Jonsson, and S. R. Carpenter. 2003. "Ecological Community Description Using the Food Web, Species Abundance, and Body Size." *Proceedings of the National Academy of Sciences of the United States of America* 100: 1781–1786. https://doi.org/10.1073/pnas.232715699.

Couret, M., J. M. Landeira, V. M. Tuset, A. N. Sarmiento-Lezcano, P. Vélez-Belchí, and S. Hernández-León. 2023. "Mesozooplankton Size Structure in the Canary Current System." *Marine Environmental Research* 188: 105976. https://doi.org/10.1016/j.marenvres.2023.105976.

Cury, P., A. Bakun, R. J. M. Crawford, et al. 2000. "Small Pelagics in Upwelling Systems: Patterns of Interaction and Structural Changes in "Wasp-Waist" Ecosystems." *ICES Journal of Marine Science* 57: 603–618.

Czudaj, S., C. Möllmann, and H. O. Fock. 2022. "Length–Weight Relationships of 55 Mesopelagic Fishes From the Eastern Tropical North Atlantic: Across- and Within-Species Variation (Body Shape, Growth Stanza, Condition Factor)." *Journal of Fish Biology* 101: 26–41. https://doi.org/10.1111/jfb.15068.

del Rio, C. M. 2008. "Metabolic Theory or Metabolic Models?" *Trends in Ecology & Evolution* 23: 256–260. https://doi.org/10.1016/j.tree.2008.01.010.

Dudeck, T., and W. Ekau. 2022. "EK60 Raw Multi-Frequency (EK80, 38 and 200 kHz) Acoustic Data Collected During RV METEOR Cruise M153 to the Benguela Upwelling System Work Area." https://doi.org/10.1594/PANGAEA.943131.

Duncan, S. E., W. Hagen, and O. H. Fock. 2024. "Mesopelagic Fish Assemblages in the Mauritanian Upwelling System Off Northwest Africa With Oxygen as a Major Driving Force." *Marine Ecology Progress Series* 733: 95–110.

Duncan, S. E., A. F. Sell, W. Hagen, and H. O. Fock. 2022. "Environmental Drivers of Upper Mesopelagic Fish Assemblages in the Benguela Upwelling Systems During Austral Summer." *Marine Ecology Progress Series* 688: 133–152.

Duncombe Rae, C. M. 2005. "A Demonstration of the Hydrographic Partition of the Benguela Upwelling Ecosystem at 26°40′S." *African Journal of Marine Science* 27: 617–628. https://doi.org/10.2989/18142320509504122.

Edwards, A. M. 2008. "Using Likelihood to Test for Lévy Flight Search Patterns and for General Power-Law Distributions in Nature." *Journal of Animal Ecology* 77: 1212–1222. https://doi.org/10.1111/j.1365-2656.2008.01428.x.

Edwards, A. M., R. A. Phillips, N. W. Watkins, et al. 2007. "Revisiting Lévy Flight Search Patterns of Wandering Albatrosses, Bumblebees and Deer." *Nature* 449: 1044–1048. https://doi.org/10.1038/nature06199.

Edwards, A. M., J. P. W. Robinson, J. L. Blanchard, J. K. Baum, and M. J. Plank. 2020. "Accounting for the Bin Structure of Data Removes Bias When Fitting Size Spectra." *Marine Ecology Progress Series* 636: 19–33. https://doi.org/10.3354/meps13230.

Edwards, A. M., J. P. W. Robinson, M. J. Plank, J. K. Baum, and J. L. Blanchard. 2017. "Testing and Recommending Methods for Fitting Size Spectra to Data." *Methods in Ecology and Evolution* 8: 57–67. https://doi.org/10.1111/2041-210X.12641.

Ekau, W. 2019. "Trophische Transfereffizienz im Benguelastrom, TRAFFIC." In *METEOR Reisen Nr. M152/2 – M153 03. 01. 2019–31. 03. 2019*, edited by Leitstelle Deutsche Forschungsschiffe, 15–21. Leitstelle Deutsche Forschungsschiffe.

Emeis, K., A. Eggert, A. Flohr, et al. 2018. "Biogeochemical Processes and Turnover Rates in the Northern Benguela Upwelling System." *Journal of Marine Systems* 188: 63–80. https://doi.org/10.1016/j.jmarsys.2017.10.001.

Fock, H. O. 2009. "Deep-Sea Pelagic Ichthyonekton Diversity in the Atlantic Ocean and the Adjacent Sector of the Southern Ocean." *Global Ecology and Biogeography* 18: 178–191.

Fock, H. O., H. Andresen, A. Bertrand, et al. 2024. "Synthetic Pelagic Biomass Size Spectra of the Tropical and Subtropical Atlantic – Biovolume and Carbon Biomass Data." https://doi.org/10.5281/zenodo.13627093.

Fock, H. O., and S. Czudaj. 2019. "Size Structure Changes of Mesopelagic Fishes and Community Biomass Size Spectra Along a Transect From the Equator to the Bay of Biscay Collected in 1966–1979 and 2014–2015." *ICES Journal of Marine Science* 76: 755–770. https://doi.org/10.1093/icesjms/fsy068.

Fock, H. O., and S. Duncan. 2024. "Mesopelagic Fishes of the Benguela Upwelling System, Cruise RV Meteor 153, 2019, and Cruise RV Sonne 285, 2021." https://doi.org/10.1594/PANGAEA.968479.

Gaedke, U. 1992. "The Size Distribution of Plankton Biomass in a Large Lake and Its Seasonal Variability." *Limnology and Oceanography* 37: 1202–1220. https://doi.org/10.4319/lo.1992.37.6.1202.

Gaston, K. J., and T. M. Blackburn. 2000. "Body Size." In *Pattern and Process in Macroecology*, 201–271. Blackwell Scientific Publications.

González-García, C., S. Agustí, J. Aiken, et al. 2023. "Basin-Scale Variability in Phytoplankton Size-Abundance Spectra Across the Atlantic Ocean." *Progress in Oceanography* 217: 103104. https://doi.org/10.1016/j.pocean.2023.103104.

Griffiths, D. 1999. "On Investigating Local-Regional Species Richness Relationships." *Journal of Animal Ecology* 68: 1051–1055.

Herring, P. 2002. *The Biology of the Deep Sea*. Oxford University Press.

Hutchings, L., C. D. van der Lingen, L. J. Shannon, et al. 2009. "The Benguela Current: An Ecosystem of Four Components." *Progress in Oceanography* 83: 15–32. https://doi.org/10.1016/j.pocean.2009.07.046.

Illig, S., and M. L. Bachèlery. 2023. "The 2021 Atlantic Niño and Benguela Niño Events: External Forcings and Air – Sea Interactions Sea Level Interannual Anomaly." *Climate Dynamics* 62: 1–24. https://doi.org/10.1007/s00382-023-06934-0.

Jarre, A., L. Hutchings, S. P. Kirkman, et al. 2015. "Synthesis: Climate Effects on Biodiversity, Abundance and Distribution of Marine Organisms in the Benguela." *Fisheries Oceanography* 24, no. S1: 122–149. https://doi.org/10.1111/fog.12086.

Jennings, S., and S. Mackinson. 2003. "Abundance-Body Mass Relationships in Size-Structured Food Webs." *Ecology Letters* 6: 971–974. https://doi.org/10.1046/j.1461-0248.2003.00529.x.

Kerr, S. R., and L. M. Dickie. 2001. *The Biomass Spectrum*. Columbia University Press.

Knorrn, A. H., H. Andresen, K. L. Wieben, and H. O. Fock. 2023. "Reproductive Biology of the Electric Lanternfish *Electrona risso*

(Myctophidae) and the Bigscale Fishes Melamphaes Polylepis and *Scopelogadus mizolepis* (Melamphaidae)." *Journal of Fish Biology* 104, no. 1: 252–264. https://doi.org/10.1111/jfb.15575.

Lindmark, M., J. Ohlberger, M. Huss, and A. Gårdmark. 2019. "Size-Based Ecological Interactions Drive Food Web Responses to Climate Warming." *Ecology Letters* 22: 778–786. https://doi.org/10.1111/ele.13235.

Liu, X., J. P. Dunne, C. A. Stock, M. J. Harrison, A. Adcroft, and L. Resplandy. 2019. "Simulating Water Residence Time in the Coastal Ocean: A Global Perspective." *Geophysical Research Letters* 46: 13910–13919. https://doi.org/10.1029/2019GL085097.

Luiz, O. J., and A. J. Edwards. 2011. "Extinction of a Shark Population in the Archipelago of Saint Paul's Rocks (Equatorial Atlantic) Inferred From the Historical Record." *Biological Conservation* 144: 2873–2881.

Mullon, C., P. Fréon, C. Parada, C. Van Der Lingen, and J. Huggett. 2003. "From Particles to Individuals: Modelling the Early Stages of Anchovy (*Engraulis capensis*/Encrasicolus) in the Southern Benguela." *Fisheries Oceanography* 12: 396–406. https://doi.org/10.1046/j.1365-2419.2003.00240.x.

Newman, M. E. J. 2005. "Power Laws, Pareto Distributions and Zipf's Law." *Contemporary Physics* 46: 323–351. https://doi.org/10.1080/00107510500052444.

Palomares, M. L. D., and D. Pauly. 2009. "The Growth of Jellyfishes." In *Jellyfish Blooms: Causes, Consequences, and Recent Advances*, 11–21. Springer.

Paternoster, R., R. Brame, P. Mazerolle, and A. Piquero. 1998. "Using the Correct Statistical Test for the Equality of Regression Coefficients." *Criminology* 36: 859–866.

Platt, T., and K. Denman. 1977. "Organisation in the Pelagic Ecosystem." *Helgoländer Wissenschaftliche Meeresuntersuchungen* 30: 575–581. https://doi.org/10.1007/BF02207862.

Price, C. A., J. S. Weitz, V. M. Savage, et al. 2012. "Testing the Metabolic Theory of Ecology." *Ecology Letters* 15: 1465–1474. https://doi.org/10.1111/j.1461-0248.2012.01860.x.

Ragoasha, N., S. Herbette, G. Cambon, J. Veitch, C. Reason, and C. Roy. 2019. "Lagrangian Pathways in the Southern Benguela Upwelling System." *Journal of Marine Systems* 195: 50–66. https://doi.org/10.1016/j.jmarsys.2019.03.008.

Rixen, T., P. Borowski, S. Duncan, et al. 2021. "SO285 Cruise Report."

Rodriguez, J., and M. M. Mullin. 1986. "Relation Between Biomass and Body Weight of Plankton in a Steady State Oceanic ecosystem1." *Limnology and Oceanography* 31: 361–370. https://doi.org/10.4319/lo.1986.31.2.0361.

Rossberg, A. G. 2012. "A Complete Analytic Theory for Structure and Dynamics of Populations and Communities Spanning Wide Ranges in Body Size." *Advances in Ecological Research* 46: 427–521.

Rossberg, A. G., U. Gaedke, and P. Kratina. 2019. "Dome Patterns in Pelagic Size Spectra Reveal Strong Trophic Cascades." *Nature Communications* 10: 1–11. https://doi.org/10.1038/s41467-019-12289-0.

Rouault, M., S. Illig, C. Bartholomae, C. J. C. Reason, and A. Bentamy. 2007. "Propagation and Origin of Warm Anomalies in the Angola Benguela Upwelling System in 2001." *Journal of Marine Systems* 68: 473–488. https://doi.org/10.1016/j.jmarsys.2006.11.010.

Rouault, M., and F. S. Tomety. 2022. "Impact of El Nino – Southern Oscillation on the Benguela Upwelling." *Journal of Physical Oceanography* 52: 2573–2587. https://doi.org/10.1175/JPO-D-21-0219.1.

Savage, V. M., J. F. Gillooly, J. H. Brown, G. B. West, and E. L. Charnov. 2004. "Effects of Body Size and Temperature on Population Growth." *American Naturalist* 163: 429–441. https://doi.org/10.1086/381872.

Sheldon, R. W., and T. R. Parsons. 1967. "A Continuos Size Spectrum for Particulate Matter in the Sea." *Journal of the Fisheries Research Board of Canada* 24: 909–915.

Sheldon, R. W., A. Prakash, and H. Sutcliffe. 1972. "The Size Distribution of Particles in the Ocean." *Limnology and Oceanography* XVII: 327–340.

Thiebaux, M. L., and L. M. Dickie. 1992. "Models of Aquatic Biomass Size Spectra and the Common Structure of Their Solutions." *Journal of Theoretical Biology* 159: 147–161. https://doi.org/10.1016/S0022-5193(05)80699-X.

Thiebaux, M. L., and L. M. Dickie. 1993. "Structure of the Body-Size Spectrum of the Biomass in Aquatic Ecosystems: A Consequence of Allometry in Predator-Prey Interactions." *Canadian Journal of Fisheries and Aquatic Sciences* 50: 1308–1317. https://doi.org/10.1139/f93-148.

Thompson, R. M., M. Hemberg, B. M. Starzomski, and J. B. Shurin. 2007. "Trophic Levels and Trophic Tangles: The Prevalence of Omnivory in Real Food Webs." *Ecology* 88: 612–617. https://doi.org/10.1890/05-1454.

Tiedemann, M., H. O. Fock, P. Brehmer, J. Döring, and C. Möllmann. 2017. "Does Upwelling Intensity Determine Larval Fish Habitats in Upwelling Ecosystems? The Case of Senegal and Mauritania." *Fisheries Oceanography* 26: 655–667.

Trebilco, R., N. K. Dulvy, S. C. Anderson, and A. K. Salomon. 2016. "The Paradox of Inverted Biomass Pyramids in Kelp Forest Fish Communities." *Proceedings of the Royal Society B: Biological Sciences* 283: 20160816. https://doi.org/10.1098/rspb.2016.0816.

Tsai, C. H., C. H. Hsieh, and T. Nakazawa. 2016. "Predator–Prey Mass Ratio Revisited: Does Preference of Relative Prey Body Size Depend on Individual Predator Size?" *Functional Ecology* 30: 1979–1987. https://doi.org/10.1111/1365-2435.12680.

Vidondo, B., Y. T. Prairie, J. M. Blanco, and C. M. Duarte. 1997. "Some Aspects of the Analysis of Size Spectra in Aquatic Ecology." *Limnology and Oceanography* 42: 184–192. https://doi.org/10.4319/lo.1997.42.1.0184.

Werner, T., C. Buchholz, and F. Buchholz. 2015. "Life in the Sea of Plenty: Seasonal and Regional Comparison of Physiological Performance of *Euphausia hanseni* in the Northern Benguela Upwelling System." *Journal of Sea Research* 103: 103–112. https://doi.org/10.1016/j.seares.2015.06.018.

White, E. P., B. J. Enquist, and J. L. Green. 2008. "On Estimating the Exponent of Power-Law Frequency Distributions." *Ecology* 89: 905–912. https://doi.org/10.1890/07-1288.1.

Williams, M. R., B. B. Lamont, and T. He. 2022. "Dealing With 'the Spectre of "Spurious" Correlations': Hazards in Comparing Ratios and Other Derived Variables With a Randomization Test to Determine if a Biological Interpretation Is Justified." *Oikos* 2022: e08575. https://doi.org/10.1111/oik.08575.

Witek, Z., and A. Krajewska-Soltys. 1989. "Some Examples of the Epipelagic Plankton Size Structure in High Latitude Oceans." *Journal of Plankton Research* 11: 1143–1155. https://doi.org/10.1093/plankt/11.6.1143.

Zhou, M. 2006. "What Determines the Slope of a Plankton Biomass Spectrum?" *Journal of Plankton Research* 28: 437–448. https://doi.org/10.1093/plankt/fbi119.

Supporting Information